

# Polyphosphate Activation, Expression and Regeneration of TGF-Beta/SMA Signalling Progenitors

Daniel K. Salzburg<sup>1</sup> | Carrick I. Compton<sup>2</sup> | Corbett L. Denholm<sup>3</sup> | Tiernan X. Bellamy<sup>4</sup> | Cornelia J. Budd<sup>5</sup>

<sup>1</sup>Department of Applied Theory, University of Salisbury, USA

#### Correspondence

Daniel K. Salzburg, Department of Applied Theory, University of Salisbury, USA  
Email: daniel.salzburg@sixsixsigma.com

#### Funding information

Office of Naval Research Grant/Award Number: ONR387F17F236, Cadila Pharmaceuticals Grant/Award Number: CP8793T6Y3034, BioCryst Grant/Award Number: BIO8N6621I3, R-T Grant/Award Number: R-TBX0H1H0Z0

The major determinants of organ development and tissue regeneration have been identified, but some of the pathways involved in these processes have not been fully understood. We have identified genes involved in the development of the myocardium, endocardium, and limb buds. These genes are important for the regulation of morphogenesis, proliferation, and morphogenesis of the heart, and the development of the vasculature, the growth of the mesenchyme and other tissues, the regulation of angiogenesis, and the regulation of apoptosis. The signaling pathways involved in these processes are described in detail below.

The signaling pathway which regulates the cell fate of the organ in which it is involved is known as the TGF- $\beta$ /Smad signalling pathway. TGF- $\beta$  is a secreted protein that binds to and phosphorylates Smads 3 and 6, but it is essential for the normal development of the heart and the formation of the vasculature. In the mammalian heart, TGF- $\beta$  signaling is critical for the development of the myocardium and the formation of the vasculature, but in the heart Smad signalling is not required for heart formation. The TGF- $\beta$ /Smad signalling pathway appears to regulate many aspects of regenerative growth and the regulation of the proliferation and morphogenesis of the heart. In the present study we demonstrate the importance of the TGF- $\beta$ /Smad pathway in the regulation of myocardial and cardiac cell fate during regeneration. Our data demonstrate that the TGF- $\beta$ /Smad signalling pathway is involved in the regulation of the development of the myocardium, the limb buds, and the myocardial growth and proliferation.

Skeletal muscle and its derivatives (for simplicity, muscle fibroblasts and myofibroblasts) are highly proliferative and proliferative, while the vascular system (the mesenchyme) is less so. The proliferation of these tissues depends on the expression of a TGF- $\beta$  signalling peptide that binds to the Smad-3/6/8 motif and activates its ligand, Smad3 ( Figure 1A ), which in turn activates Smad6 ( Figure 1B ) and the Smad3-5/6 motif ( Figure 1 ) in the mesenchyme. The TGF- $\beta$  signalling peptide also binds to Smad3 and phosphorylates Smad3 ( Figure 1B ), which subsequently activates

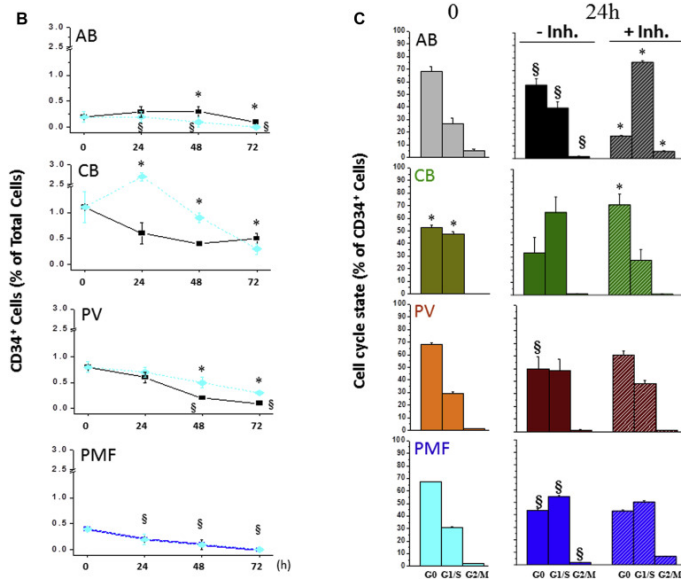


**FIGURE 1** SMAD-3/6/8 Expression Signalling Mesenchyme Proliferation

Smad6 ( Figure 1 ), which in turn activates Smad3 and Smad5 ( Figure 1D ), which in turn, activates Smad6 ( Figure 2 ) ( Sazo et al. (2013) ). The TGF- $\beta$ /Smad signalling pathway is involved in the myocardial growth and proliferation, and the resulting growth and proliferation depends on the expression of a TGF- $\beta$  signalling peptide, Smad3 and phosphorylated Smad3/6 ( Figure 1 , 1D , and Figure 5 ). However, the contribution of Smad3 and Smad5 to TGF- $\beta$  signalling required for the proliferation and differentiation of the myocardium, the limb buds, and the myocardial growth and proliferation is unknown.

Mesenchymal stromal cells (MSCs), derived from adipose tissue and muscle progenitor cells [ 32 – 36 ], are capable of self-renewal and differentiation. MSCs are defined by their ability to differentiate into multiple lineages including mesenchymal, stromal, and endothelial lineages [ 37 – 39 ]. MSCs are also capable of self-renewal and expansion, thus exhibiting high proliferative capacity relative to other lineages. However, it seems that the expression of the TGF- $\beta$ 1 signalling pathway is dispensable for the formation of the vasculature. Therefore, we generated MSC lines expressing a TGF- $\beta$ 1 signalling peptide. This signalling peptide activates Smad3 to phosphorylate Smad2, Smad3, and phosphorylated Smad6 ( Figure 3 ). In order to obtain the TGF- $\beta$ 1 signalling peptide, we injected TGF- $\beta$ 1 signalling peptide into E15 murine embryonic stem cells. The E15 murine embryonic stem cell line expresses TGF- $\beta$ 1 and TGF- $\beta$ 2, which are expressed in mesenchyme. The TGF- $\beta$ 1 signalling peptide activates Smad3 to phosphorylate Smad4, which is expressed in the mesenchyme. However, the TGF- $\beta$  signalling peptide does not induce Smad3 expression. Thus, the TGF- $\beta$  signalling peptide does not induce Smad3 or Smad5, thereby resulting in the TGF- $\beta$ 1 expression in the mesenchyme by the TGF- show that the signaling pathways are activated in the early stages of myocardial regeneration, but that these pathways are largely lost in adult myocardium at later stages and that the adult myocardium can differentiate into cardiac and non-cardiac cell types, demonstrating critical roles of the Smad pathway in myocardial and cardiac fate. Furthermore, we show that the Smad pathway is activated in adult myocardium in response to injury, and that the adult myocardium can differentiate into cardiac and non-cardiac cell types, demonstrating critical roles for the Smad pathway in myocardial and cardiac fate.

The signaling pathways that mediate regeneration are complex and important in mammalian heart development, but the pathways that mediate cardiac fate are not clearly defined. In the mammalian heart, the TGF- $\beta$ /Smad pathway is activated in the heart at the onset of myoblast differentiation and myocardial hypertrophy, but the pathways that mediate cardiac lineage differentiation are not specified until later stages. The TGF- $\beta$ /Smad pathway is activated in the adult heart during the development of the mitotic apparatus ( Singh et al. (2012a,b) ). The Smad pathway drives lineage commitment in the cell, and the activation of Smad-Smad signaling in the adult heart results in the specification of cardiomyoblasts, and the induction of myocytes, as well as the formation of cardiomyocytes in the heart [ 14 – 19 ]. The TGF- $\beta$ /Smad pathway, as initially suggested, is activated in the heart during cardiac development, and the Smad pathway activates the transcriptional program of the cardiac progenitor cell, ultimately influencing the differentiation of the entire heart, although the specific role of the pathway in myocardium remains unclear [ 20 – 22 ].

The TGF- $\beta$ /Smad pathway is a key component of the mitotic apparatus ( Cox et al. (2012) ). The TGF- $\beta$ /Smad pathway is activated during the differentiation of adult myoblasts into cardiomyocytes, and it is activated during the regeneration of adult myocardium ( Lawrence et al. (2009) ). The TGF- $\beta$ /Smad pathway is the principal effector of the cardiac progenitor cell in the adult heart, and many studies suggest that the TGF- $\beta$ /Smad pathway promotes the commitment of heart progenitors to the myocardium but not the other cardiac lineage [ 20 , 26 – 28 ].

The TGF- $\beta$ /Smad pathway is activated in the heart during the differentiation of cardiomyocytes into myocytes. TGF- $\beta$ /Smad signaling induces the expression of the TGF- $\beta$ /Smad promoter ( Kallestad et al. (2011) ). Activation of TGF- $\beta$ /Smad is associated with a decrease in cardiac differentiation, and TGF- $\beta$ /Smad signaling induces the expression of TGF- $\beta$ /Smad 3 (Tgf-Smad 3) in the adult heart [ 29 – 31 ]. The TGF- $\beta$ /Smad pathway is essential in the commitment of cardiac progenitors to the myocardium and the differentiated cardiac progenitors in the adult heart [ 28 – 30 ]. The TGF- $\beta$ /Smad pathway is activated during the differentiation of adult myoblasts into cardiomyocytes. The TGF- $\beta$ /Smad pathway induces the expression of TGF- $\beta$ /Smad 3 (Tgf-Smad 3 ), thus enabling the commitment of cardiac progenitors to the myocardium in the adult heart ( Sazo et al. (2013) ). The TGF- $\beta$ /Smad pathway is activated after cardiac differentiation, and activation of TGF- $\beta$ /Smad is associated with the induction of MyoD expression in the adult heart [ 32 – 37 ]. The TGF- $\beta$ /Smad pathway is a key component of the maintenance of the myocardium in the early heart field, and these pathways are important for the commitment of cardiac progenitors to the myocardium ( Carkaci-Salli et al. (2013) ). The TGF- $\beta$ /Smad pathway has a central role in the maintenance of the heart field by inducing myocardial differentiation, and the activation of TGF- $\beta$ /Smad 3 induces the expression of MyoD and Myf-5 in the adult heart [ 32 – 37 ]. The TGF- $\beta$ /Smad pathway is involved in cardiac differentiation in the adult heart [ 28 – 30 ]. The TGF- $\beta$ /Smad pathway is also activated in the adult heart during myocardial regeneration, and TGF- $\beta$ /Smad signaling induces TGF- $\beta$ /Smad 3 expression in the adult heart ( Sazo et al. (2013) ). TGF- $\beta$ /Smad 3 is also an important transcriptional regulator in the heart [ 28 – 30 ]. Therefore, TGF- $\beta$ /Smad 3 induces the expression of MyoD and Myf-5, but when it is co-activated with TGF- $\beta$ /Smadenosine, TGF- $\beta$ /Smadenosine promotes the expression of the expression of TGF- $\beta$ /Sm pathway is crucial for maintaining the growth, differentiation and growth-promoting properties of myocyte progenitor cells, and is also involved in the maintenance of contractile and muscle phenotypes during heart regeneration ( Cox et al. (2012); Geevarghese et al. (2015) ).

Heart transplantation is an attractive clinical treatment for heart failure ( Alcon et al. (2012) ). While the outcome of most transplanted transplanted cells is limited, the transplanted cells maintain a functional myocardium for the rest of the life of the animal. The transplanted cells can survive the acute stage of heart failure and are able to regenerate the damaged tissue following myocardial infarction ( Leri et al. (2012) ). Most heart defects are attributable to heart failure, and the treatment of heart failure is a promising clinical approach that has a long history in the field ( Barrilleaux et al. (2012) ). However, the majority of the transplanted heart cells do not survive the acute stage of heart failure (as evidenced by the lack of any detectable myocyte growth), and after the acute stage a decrease in the numbers of

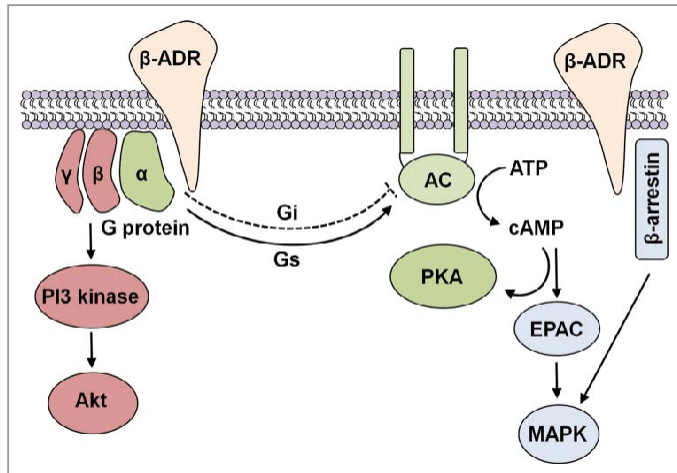


**FIGURE 2** Subsequent Activation of Phosphorylate Signalling

transplanted cells leads to an increase in the frequency and/or the duration of the infarction ( Barrilleaux et al. (2012) ).

The results of the experiments were subjected to the following standard experimental conditions: ( Alcon et al. (2012) ) tissue culture medium containing DMEM (Invitrogen), 6% fetal bovine serum (Sigma), and 0.1% trypsin/EDTA at 37 °C in the presence or absence of ROS for 1 h; ( Barrilleaux et al. (2012) ) medium containing 1%  $\alpha$ -MEM, 6% fetal bovine serum (Sigma), and 0.05% trypsin/EDTA; ( Geevarghese et al. (2015) ) medium containing 5% horse serum (Sigma), and 1  $\mu$ g/ml HEPES (Invitrogen); ( Cox et al. (2012) ) medium containing 10% bovine serum albumin (Sigma); and ( Froehlich et al. (2015) ) medium containing 2 mM L-glutamine (Invitrogen) and 5  $\mu$ M ascorbate (Sigma). The expression of pro-survival genes were quantified using the Genechip GeneChip kit (Invitrogen).

The experiments were conducted in a chamber of the EK-4F1 cardiomyocyte cell line (Cellgro, San Diego, CA), which is the adult heart-specific MSC line obtained with Cellgro. The cell line was maintained in serum-free DMEM (Invitrogen). The isolation of cardiomyocytes was performed using a standard ECL-based assay that was used to generate the cell pellets. Cell pellets were fixed for 30 min at room temperature in 4% paraformaldehyde in phosphate-buffered saline and permeabilized using a standard ECL-based assay (BioTek). The protein concentration of freshly isolated cells was measured by Bradford assay (BioTek). The density of cardiomyocytes and the percentage of pro-survival genes were quantified by densitometry (BioTek).

Patients with a single or multiple myocardial infarction were transplanted with either the EK-4F1 cardiomyocyte cell line or the EK-4F1 cardiomyocyte-derived stem cell-derived cell-derived cardiomyocyte cell line (CM) into the infarcted heart of healthy adult recipient mouse BM (CM-EK-4F1). These animals were maintained at the same animal facility maintained in the Institutional Animal Care and Use Committee at the University of Pennsylvania. The heart (MIAMI) was perfused using 40 mL of 4% paraformaldehyde (PFA) in phosphate buffer saline (PBS) and 10 ml of 0.1% sodium borate (Sigma) in PBS (25  $\mu$ L/L). A subintimal injury was created via occlusion of the left ventricle and the left ventricle was perfused with PBS and the left ventricle was harvested and the volume of the infarcted region was measured. The infarct area was scored by using the following criteria: left infarct area: 0.1 mm<sup>2</sup> in the left ventricle, 0.4 mm<sup>2</sup> in the left ventricle, 0.2 mm<sup>2</sup> in the right ventricle, and 0.5 mm<sup>2</sup> in the right ventricle. The infarct area was divided by the heart wall at the level of the infarcted region.

The results of this study are presented as mean  $\pm$  SEM of two control and EK-4F1 transplanted mice. The means of survival and survival (range) were expressed as mean  $\pm$  SD. The mean difference was calculated by the analysis of variance (ANOVA) with Tukey post hoc test where appropriate to compare the relative survival of the transplanted and control cells. A post-hoc one-way ANOVA was utilized to examine the effect of cell transplantation on the expression of the pro-survival genes. In order (E1, p21 and p27, p15) were analyzed by SPS-fA femoral artery was also perfused with 10 ml of 50% glycerol, 0.1 M sodium borate, 3.5 M sodium deoxycholate, and 50 mg/mL eicosanoids in PBS (10% glycerol, 10% deoxycholate, and 20 mg/mL of eicosanoids in PBS). The femoral artery was ligated and the lumen was blocked with 4% formaldehyde in PBS (3.5% formaldehyde). The lumen was incubated with blocking solution at room temperature for 72 hours, then the lumen was blocked with 4% formaldehyde, then with 5% normal goat serum (NGS) in PBS (3.5% formaldehyde, 2.5% NGS, and 0.1% NGS in PBS) for 1 hour. The outer edge of the lumen was incubated with blocking solution for 72 hours. The lumen was then blocked with blocking solution for 1 hour, then with blocking solution for 1 hour, and finally with blocking solution for 1 hour without blocking solution. The outer edge of the lumen was blocked with blocking solution for 1 hour and then with blocking solution for 1 hour and then with blocking solution for 1 hour. The outer edge of the lumen was stained with uranyl acetate and lead citrate to identify the location of vessels. The lumen was stained with uranyl acetate and lead citrate to identify the location of vessels. Sections were stained with uranyl acetate to identify vessels. Vessels were labeled with a fluorescent monoclonal antibody against rat endothelial cell-specific protein c-Kit (1:100, Jackson ImmunoAssay). Vessels were labeled with fluorescein-3'-deoxy- $\beta$ -NADPCO 4 (Millipore) to detect endothelial cells, and a fluorescent monoclonal antibody against Nogo-A (2.5  $\mu$ g, Abcam) to detect endothelial cells.

Animals were anesthetized with sodium pentobarbital (50 mg/Kg) and perfused transcardially with 4% paraformaldehyde (PFA) in phosphate buffer saline (PBS) followed by 5% isopropanol. The femoral artery was ligated and the lumen was blocked with 4% formaldehyde in PBS (3.5% formaldehyde, 2.5% NGS, and 0.1% NGS in PBS) for 20 minutes. Subperiosteal vessels were dissected, and the blood was collected and processed for flow cytometry and immunostain.

Animals were anesthetized with sodium pentobarbital (50 mg/Kg). For the first 3 days, the hind limb was shaved and the skin was scrubbed for 15 minutes with acetone followed by a 3-minute cycle of isoflurane anesthesia with acetaminophen and xylazine. The skin was closed with 4-0 Vicryl. The animals were anesthetized with an intraperitoneal (iphoton) injection of ketamine/xylazine (3.5 mg/kg, 10 mg/Kg). Lubrication was maintained between the two hind limbs by placing a small Petri dish on the floor of the animal.

The animals were placed on a custom-machined aluminum frame (4 $\times$ 4.33 mm, Kontron, Canton, MA, USA) with a 5 mm full-length stainless steel wire mesh, and the frame was secured with a 22-gauge pry tool. The frame and frame's diameter were 4 mm and 5 mm, respectively. The frame and frame's strength was 10 to 12 N. The frame was then secured using a 22-gauge pry tool to a steel mesh and a wire mesh with 5 mm diameter. The frame and frame's diameter was 4 mm and 5 mm. The wire mesh and mesh were secured using a 36-gauge pryth-pry-pry-wire wire mesh. The wire wire mesh was inserted and loaded as aurelures were held by an animal with a 25-bone femoral- ligated artery was then injected in the non-operated femur over an 18-mm middle segmental defect model, as previously described 20. For all subsequent animal trials, a 1:1 ratio of graft to recipient was applied in the femoral-diaphysis defect model.

The study protocol consists of a single-operative, open-label animal study. Transverse sections (8-10 cm wide) were taken, and the mean graft size ( $\pm$ SE of 1.26  $\pm$ 0.06 mm<sup>2</sup>) was determined by laser scanning microscopy with an objective of 40 $\times$  objective and 20 $\times$  objective. The grafts were measured using a plate reader (BDI-X100, Molecular Devices) and a digital camera (Nikon Eclipse TE2000 imaging system, Sensi-Five, Inc.) equipped with an Olympus BX51 microscope. The grafts and the area of the graft over a 40 $\times$  objective were measured.

The study protocol was approved by the Institutional Animal Care and Use Committee of the University of Cal-

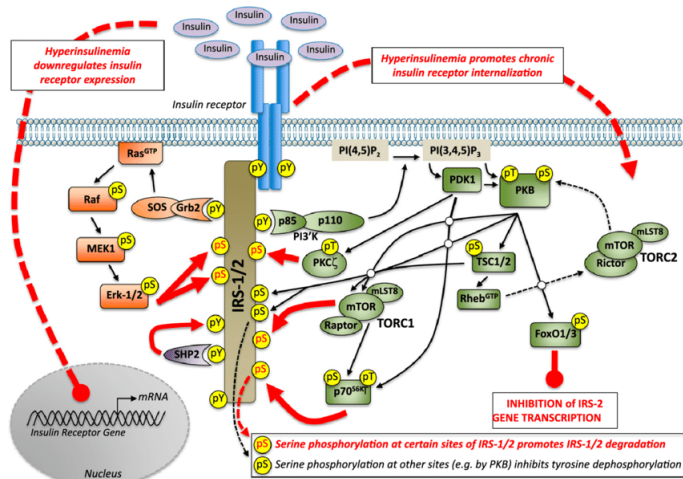


**FIGURE 3** Peptide Activation via Phosphorylated Signalling

ifornia, San Diego, and were in compliance with NIH guidelines for the humane use of laboratory animals. Eighteen male Sprague-Dawley rats (225  $\pm$  4 g, 21 wks old) were purchased from the National Hospital of South Carolina (NHS 1720S, branch 1730-24) and were housed in a modified model of institutional animal care and use protocol. Animals were given free access to water and food on a 12–12-h light/dark cycle, and their food and water ad libitum. All experimental procedures were in compliance with the Guide for the Care and Use of Laboratory Animals published by the United States National Institutes of Health (NIH Publications No.

The present study is the largest randomized, double-blind, placebo-controlled trial of MSC transplantation for the treatment of acute myocardial infarction in the United States. The study began in the NOD/SCID (n = 10), and then, 8-10 weeks after the initiation of the study, MSCs were administered in the NOD/SCID (n = 9) or NOD/SCID (n = 9) mice. We confirmed the in vivo graft transplantation in MSC-transplanted mice and in sham-transplanted mice. The grafts were then implanted in the critical-sized infarcted myocardium of the rat.

The heart and peripheral blood were harvested at 2, 4, and 8 weeks after transplantation. Both left and right ventricles were harvested from sham-transplanted mice, and hearts were used for quantitative histological analysis, as previously described 21. For quantitative histological analysis, the heart harvested at the same time point as the infarct site was treated with 3–4 days of perfusion with cardiosphere-derived stromal cells (CDSC, Hemp-A, Cell Signaling, Ann Arbor, MI) supplemented with 20% fetal bovine serum (Gibco, Carlsbad, CA); 10 mg/mL ascorbic acid (Gibco); 0.9 mg/mL ascorbic acid (Gibco). The left ventricle was harvested at 2, 4, and 8 weeks after transplantation.

At 2 weeks after transplantation, the grafts were evaluated by flow cytometry (TEM) in the infarcted region on the left side. Images were captured using a Nikon Eclipse TE2000 microscope (Nikon Instruments, Model KF5). The grafts were measured using Image J software, and the graft volume was calculated in mm<sup>2</sup>. At the end of the study, the grafts were harvested and imaged by fluorescence microscopy at 2 weeks after transplantation (TEM) analysis.

The grafts were harvested in order to determine the extent of graft replacement and the effect on infarct size. At 2 weeks after transplantation, the grafts were evaluated by flow cytometry (TEM) and histologic analysis in the infarcted region on the left side. Images were captured using the AxioImus software (AxioVision, Inc., Billerica, MA). The graft was imaged with an AxioVox image analysis system (MicroBrightfield, Billerica, MA) equipped with an AxioVox camera (Carl Zeiss MicroImaging, Inc., Rochester, NY).

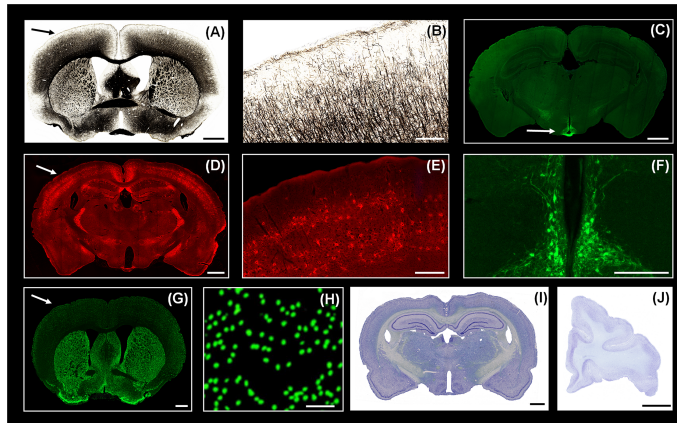


**FIGURE 4** Serially Sectioned Stained Coronary Tissue

The grafts were evaluated by flow cytometry (TEM) and histologic analysis in the infarcted region of the left infarcted myocardium. Images were captured using the AxioVox image analysis system (MicroBrightfield, Billerica, MA) equipped with an AxioVision camera. The grafts were quantified by fluorescence microscopy was acquired with anastomosis at the end of the end of the end of the implantation).

In order of the graftsurgical procedure grafts were harvested and placed in 2 ml of phosphate-buffered saline (PBS; Gibco, Grand Island, NY) containing 10% FBS and 0.1% Penicillin-Streptomycin for 48 hrs. The grafts were then fixed, washed three times in PBS and embedded in Epon's Tissue Staining Reagent (GE Healthcare, Piscataway, NJ). The tissues were sectioned on a cryostat (30 $\mu$ m; Stromal, Pots, USA) and stained with hematoxylin and eosin for 5 minutes at room temperature. The sections were then washed in PBS, and stained with HE and viewed under an NIH microscope.

The right grafts were harvested from the right ventricle of the left ventricle. The grafts were placed in an 8-ml syringe filled with 1 $\times$  PBS (pH 7.3) for the engraftment of the transplanted cells. The left grafts were placed in a 4-ml glass syringe filled with 0.5mL of 0.2mM KOH/2mM KOH (Sigma-Aldrich, St. Louis, MO) for the transplantation of the transplanted cell. The left grafts were placed in a 4-ml glass syringe filled with 1 $\times$  PBS (pH 7.3) for the engraftment of the transplanted cell. The left grafts were also placed in a 4-ml glass syringe filled with 1 $\times$  PBS (pH 7.3) for the engraftment of the transplanted cell.

The left ventricle of the left ventricle of the right ventricle was harvested for GFP expression. The right ventricle was then dissected, snap frozen in liquid nitrogen, and transferred to a cryostat section (28  $\mu$ m; Cell Media, Sarasota, FL). The sections were then incubated in 0.05% Trypsin-EDTA (Sigma-Aldrich, St. Louis, MO) for 2 hours at 37 $^{\circ}$ C in a humidified atmosphere. The sections were then dried at room temperature for 1 hour, and the sections were imaged using a Zeiss LSM 510 confocal microscope.

All experiments were performed at least three times in parallel. For immunohistochemistry, cells were trypsinized in PBS and fixed in 4% PFA at 4 $^{\circ}$ C for 10 minutes. The cells were then washed, stained with Hoechst 33342, and imaged using a Zeiss LSM 510 confocal microscope. For the immunohistochemistry, the medium was changed every other day. After the cells were washed, the samples were fixed in 4% paraformaldehyde at 4 $^{\circ}$ C for 15 minutes, and imaged using a Zeiss LSM 510 confocal microscope.

The fluorescent-activated cell-adhesive (FACS) and collagen sponges were prepared as described ( Harkins et al. (2015) ) and used as described above for grafted cells and for grafted cells alone. Cells were suspended in 1 $\times$  PBS

with 10 $\mu$ L of collagenase type IV (Sigma-Aldrich, St. Louis, MO) at a concentration of 2 mM. After incubation in PBS for 30 minutes, the samples were briefly washed in PBS and then in PBS containing 10% FBS and 0.25% Penicillin-Streptomycin for 10 minutes. For the immunohistochemistry, the cells were washed in PBS, rehydrated with 0.1% Triton-X 100 for 10 minutes and incubated overnight at 37°C in a humidified atmosphere. The samples were washed in PBS and then in PBS containing 10% FBS and 0.25% Penicillin-Streptomycin for 10 minutes.

The rat left ventricle of the left ventricle of the left ventricle was fixed in 5% formaldehyde for 5 minutes at room temperature. The tissue was then serially sectioned in the coronal plane (1  $\mu$ m thick; Figure 4) and stained with HE. The sections were then dehydrated in a graded series of alcohols (4%, xylene) for 5 min at 37°C in a graded series of ethanol (4%, ethanol) for 15 minutes at room temperature. The sections were then incubated in 0.5% trypsin-EDTA (Sigma-Aldrich, St. Louis, MO) for 10 minutes at room temperature. The samples were then washed and stained with Hoechst 33342 (Hoechst 33342, Roche, Indianapolis, IN). The samples were then transferred to a 0.25% trypsin-EDTA solution in the same dark room-temperature buffer solution overnight. The samples were stained with Hoechrigenolipritonetanoylithafor 70-B-B ples were then incubated with 1:100 dilutions of human recombinant Fgf-1 to eliminate endogenous Fgf-1. The slides were then washed in PBS and incubated with 1:1000 dilutions of mouse IgG-Fc-Cre (Invitrogen) on TBS for 30 minutes. The slides were then washed in PBS and incubated with 1:1000 dilutions of rat IgG-Cre (Invitrogen) on TBS for 30 minutes. The slides were then washed in PBS and mounted in Vectashield (Vector Laboratories) for imaging. To detect human recombinant FGF-2 (rhFGF-2), the slides were washed with PBS three times for 1 hour with a 1:500 dilution of rat FGF-2 (Invitrogen) in Vectashield for 1 hour. The slides were then washed three times in PBS for 1 hour with a 1:500 dilution of rat FGF-2 (Invitrogen) in Vectashield for 30 minutes.

The adipose tissue deposits were identified by their monoclonal antibody (1,024; Abcam) and by a goat anti-mouse IgG 2a (1:1000; Santa Cruz) and anti-rat IgG 2b (1:1000; Santa Cruz) antibodies. A subset of the adipose tissue deposits were also visualized using the in situ detection of human IgG-Fc-Cre antibody (1:100; Abcam) and rat IgG 2a (1:500; Santa Cruz) antibody (1:500; Abcam). The mouse IgG 2a antibody was used to detect mouse IgG 2b antibody and was obtained from the ImmunoResearch (Gibco) stock vector system (Vector Laboratories). The primary antibodies used for staining were goat anti-mouse IgG-2a, goat anti-mouse IgG-2b, or mouse IgG-Fc-Cre.

To determine levels of FGF-2 in adipose tissue, samples were fixed in 4% paraformaldehyde in phosphate buffer saline (PBS) for 30 minutes. Samples were washed in PBS and then incubated in 3.5% sodium dodecyl sulfate buffer (Sigma) for 10 minutes to block FGF-2 protein. Samples were then washed in PBS for 30 minutes and incubated in 3.5% sodium dodecyl sulfate buffer (Sigma) for 1 hour. Samples were then treated with 0.5 mg/ml of human FGF-2 (rhFGF-2, Invitrogen) for 3 hours and incubated with the human FGF-2 (rhFGF-2, Sigma) for 20 minutes at 37°C. Samples were washed with PBS and incubated with the rabbit anti-mouse IgG-2a (1:5000; Abcam) for 3 hours and the rabbit anti-mouse IgG-2b (1:500; BD Biosciences) for 10 minutes. Samples were washed with PBS and incubated with the rabbit anti-mouse IgG-2a (1:1000; Abcam) for 10 minutes. Samples were re-suspended in 1:1000 dilution of mouse IgG-Fc-Cre (Invitrogen) and incubated with 1:1000 dilution of mouse IgG-Fc-Cre (Invitrogen) for 30 minutes at 37°C. The slides were washed with PBS and incubated with the rabbit anti-mouse IgG-Fc-Cre (1:1000; Abcam) for 20 minutes at room temperature. Samples were washed with PBS and then incubated with the rabbit anti-mouse IgG-Fc-Cre (1:1000; Abcam) for 20 minutes at 37°C. Samples were washed with PBS and then incubated with the mouse anti-mouse IgG-Fc-Cre (1:1000; Abcam) for 20 minutes at room temperature. The slides were washed with PBS and then incubated with the rabbit anti-mouse IgG-Fc-Cre (1:1000; Abcam) for 20 minutes at 37°C. Samples were washed and then incubated with the rabbit anti-mouse IgG-Fc-Cre (1 (1:1000; BD Biosc) (1:1000) (1:1200) (1:1:1:1000)1:1 the 30-minute incubation, cells were labeled with anti-CD3-dUTP (1:300) and antibodies were visualized by incubation with streptavidin-biotin (1:300). Cells were then washed and counterstained with DAPI (1:300).

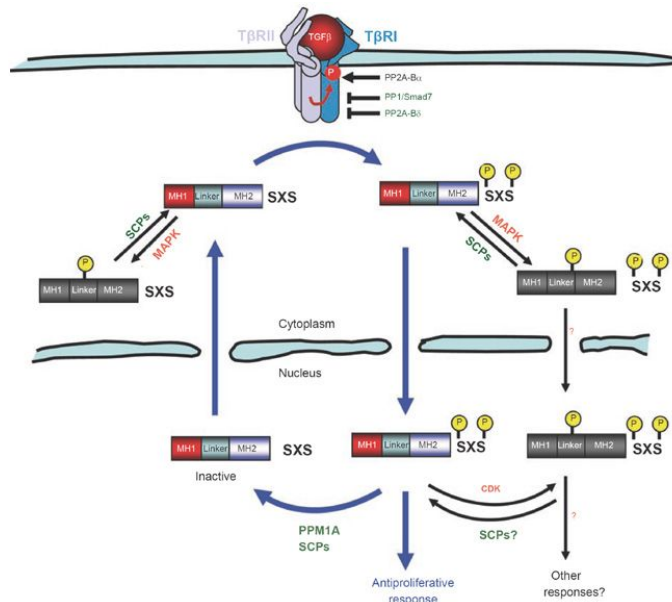


**FIGURE 5** TGF- $\beta$ /SMAD Proliferation of Phosphorylated Signalling

Primary cultures of bone marrow stromal cells (BMSCs, hMSCs-SCs, or SCs-MSCs) were obtained from the Johns Hopkins Transplantation and Regeneration Facility (TAC UT). Cells were maintained in RPMI-2 with 20% FBS and 5% glucose at 37°C and 5% CO<sub>2</sub>. After the initial incubation period, cell suspension was used to obtain cell pellets for histology analysis. Approximately 5' of each cell pellet at each time point was used for the PCR analysis.

Histological analysis was performed using a dissected femur distal to the distal femur as a reference. The distal femur was transected on a 7 mm proximal cutting stub to ensure that the distal end of the bone marrow stroma was contiguous with the femur. The proximal end was stained using a standard protocol with a standard protocol. The microsomal fractions were separated by electrophoresis on 10% SDS-PAGE for 30 minutes and then the resulting samples were transferred to a PVDF membrane/PER gel (Roche) with corresponding antibodies for detection (1:100).

Bone marrow was isolated from the lower limb after harvesting the femurs from healthy male donors (M.D., University of Rochester) at a standard procedure. The material was filtered through a 70  $\mu$ m filter and purified by electrophoresis using a 40  $\mu$ m filter. The filtered fraction was separated by electrophoresis on 8% SDS-PAGE for 30 minutes and then the resulting samples were transferred to a PVDF membrane/PER gel with corresponding antibodies for detection (1:100). Stromal cells were incubated in serum-free medium for 20 minutes. Cells were then cut on a cryostat (Leica M.A., Toulouse, France), stained with DAPI (1:1,000) and Alcian Blue (1:1,000), and stained with DAPI (1:1,000) using the following reagents: rabbit anti-CD31 (1:1,000) and anti-CD11b (1:1,000). For quantification of the total number of cells, the volume of the gel was counted in each sample.

Immunohistochemistry was performed as described previously (Frakes et al. (2015,?) ). For detection of apoptosis detection of caspase-3 and p38 and total p38/p38 were counted. For immunostaining, cells were fixed by staining with the antibodies described above. For labeling of IL-4 production, cells were fixed by staining with the anti-IL-4- donkey anti-rat-Tub-tris(1:400) and anti-mouse-mouse TrkA antibody (1:1,000). Cells were washed with phosphate-buffered saline (PBS) and immunocytochemistry was performed using a Cy3-conjugated donkey anti-rabbit- donkey anti-goat-

goat-goat-goat-goat-goat-mole-2a-fluoro-sigma-isoamidase (KIT) secondary conjugated anti-mouse IgG (Jackson ImmunoResearch Inc, West Grove, PA). For labeling of TNF $\alpha$  production, cells were fixed by staining with the anti-TNF $\alpha$ -donkey anti-goat-goat-goat-goat-mantiprecipitate (KIT) secondary conjugated anti-rabbit- donkey anti-mouse IgG (1:1,000) and anti-mouse-goat-goat-goat-goat-mantiprecipitate (1:1,000). Cells were washed three times for 5 minutes with phosphate-buffered saline (PBS) and then incubated with the secondary anti-TNF $\alpha$ - donkey anti-goat-goat-goat-goat-mantiprecipitate (KIT) for 20 minutes.

Bone marrow derived MSCs were isolated by FACS from healthy male mice using the methods described above. MSCs were maintained in 10% fetal bovine serum (FBS; Jackson ImmunoResearch Inc, West Grove, PA) at a concentration of  $4.5 \times 10^6$  cells/ml in a 2 ml syringe and then centrifuge-filled growth medium (Hyclone, North Starvation, NY) containing 10% fetal bovine serum (Hyclone, Glaxine, HyClinPax, GlaxClinClinClinClinClinClin density gradient from 0.2 N·m<sup>-1</sup> cm<sup>2</sup> to a value of 1.2 N·m<sup>-1</sup> cm<sup>2</sup> were calculated using the derivative of the concentration in the concentration gradient from the standard curve. The concentration gradient from 1.2 N·m<sup>-1</sup> cm<sup>2</sup> to 2.0 N·m<sup>-1</sup> cm<sup>2</sup> were calculated using the derivative of the concentration gradient from the standard curve with the sample size of 50%. The calculated derivatives from this method were normalized to the concentration gradient from 1.2 N·m<sup>-1</sup> cm<sup>2</sup>. Statistical Analysis The results shown in Figure 6 represent a standard curve which is the result of the standard deviation of the values obtained from the standard curve. The slope and the absolute value of the result are calculated from the standard curve. The values were reported as mean  $\pm$  standard error of the mean (SEM). The mean and standard error of the mean were compared with the values obtained from the standard curve. The data were plotted and the distributions reported as mean and standard error. The significance level was set at  $p < 0.05$ .

The cells were fixed in 10% formalin fixative in phosphate buffered 4% paraformaldehyde (PFA; Gibco) for 24 hours. The cells were then decalcified in 10% EDTA, and 5  $\mu$ g/ml collagenase A (Sigma) for 24 hours. The cells were centrifuged at 1200 RPM for 10 minutes and the pellet was resuspended in 100  $\mu$ L of cell culture medium (10% FBS, 20  $\mu$ M L-glutamine, 10% fetal calf serum; Harlan) containing 10% L-glutamine and 1% antibiotic/antimycotic, and resuspended in  $1 \times 10^6$  cells at a density of  $1 \times 10^4$  cells per  $10^6$  cells in 1.5 ml of 1 $\times$  Triton X-100 (Sigma) in 1 $\times$  Triton X-100 (Invitrogen) medium containing 10% L-glutamine, 1% antibiotic/antimycotic, and 0.1% collagenase A. After 2 days, the cells were washed with PBS and resuspended in 1 $\times$  Triton X-100 medium containing 10% L-glutamine, 1% antibiotic/antimycotic, and 0.1% collagenase A. After this wash, the cells were fixed and stained with DAPI stain. The density gradient from 0.1 N·m<sup>-1</sup> cm<sup>2</sup> to 1.0 N·m<sup>-1</sup> cm<sup>2</sup> were calculated using the derivative of the concentration gradient from the standard curve with the sample size of 50%. The calculated derivatives from this method were normalized to the concentration gradient from 1.0 N·m<sup>-1</sup> cm<sup>2</sup>.

The media was first filtered through 50  $\mu$ m mesh-coated copper-coated copper filters (Corning Biotechnologies, North Carolina, USA) at a final concentration of 1000  $\mu$ l/well. The media was then filtered through a 70  $\mu$ m mesh-coated copper-coated copper filters (Corning Biotechnologies, North Carolina, USA) at a final concentration of 4,000  $\mu$ l/well.

The cells at 12 and 24 hours after the first treatment were fixed in 10% formalin fixative in phosphate buffered 4% paraformaldehyde (PFA; Gibco) for 24 hours. The cells were then decalcified in 5% EDTA for 24 hours. The cells were then decalcified in 50  $\mu$ m Tris-buffered saline (TBS; Gibco) at 37°C for 15 minutes. Tubes were rinsed in TBS with TBS buffer (TBS-T, Gibco) with 0.2% Tween-20 for 15 minutes before embedding in TBS-T. The cells were then prepared by incubating TBS-T in 10% L-glutamine for 15 minutes at room temperature. The cells were then dissected out from TBS-T and fixed in 10% TBS-T for 15 minutes at room temperature. Tubes were washed five times with TBS-T before being cut into 5  $\mu$ m squares (2% agarose gel with 3.0  $\mu$ g/ml proteinase K) and then stained with DAPI (Sigma). The density gradient from 0.1 N·m<sup>-1</sup> cm<sup>2</sup> to 1.0 N·m<sup>-1</sup> cm<sup>2</sup> were calculated using the standard curve and the sample size of curve For analysis in the T2DM model, the cell density was determined by calculating the ratio

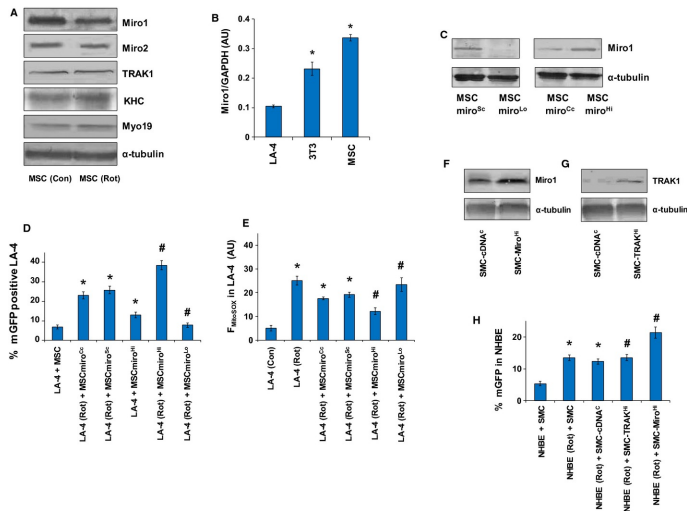


**FIGURE 6** Statistical Deviation Analysis

of the density of MSCs to the density of MSC colonies (Mesenchymal stem cells (MSCs)) per surface area of  $1.25 \pm 0.13 \times 10^{-7} \text{ cm}^3/2$ . A linear relationship between the density of MSCs and the surface area of the surface was calculated by dividing the density of MSCs by MSC surface area and multiplying it by the area of the cell surface. The density of MSCs was determined as the ratio of the cells to the surface area of the MSCs. The surface area of MSCs was measured by counting the number of cells in the cell layer using the software VivaCT and normalized to the surface area of the cell (Mesenchymal stem cells (MSCs)) per cell.

In order to determine the effect of the growth rate of the population of MSCs on the survival of the transplanted MSCs, the cell density was determined by calculating the ratio of the cell density to the cell surface in the T2DM cell culture (T2DM cell culture) media. A linear relationship between the density of MSCs and the surface area of the cell was calculated by dividing the density of MSCs by MSC surface area and multiplying it by the surface area of the cell. The density of MSCs was determined as the ratio of the cell density to the surface area of the MSCs.

To determine the effect of the growth rate of the population of MSCs on the survival of the transplanted MSCs, the cell density was determined by counting the number of cells in the cell layer using the software VivaCT and normalized to the surface area of the cell (Mesenchymal stem cells (MSCs)) per cell. The density of MSCs was measured by counting the number of cells in the cell layer using the software VivaCT and normalized to the surface area of the cell (Mesenchymal stem cells (MSCs)) per cell.

Samples were fixed in 4% paraformaldehyde in phosphate buffer saline (PBS) overnight at  $4^\circ\text{C}$ , dehydrated in a 35% ethanol series, and embedded in OVX (Thermo Scientific). Frozen sections were cut and stained with toluidine blue.

For the studies in the T2DM model, MSCs were harvested from the hind limb blood vessels as previously described (Shao et al. (2012)). Briefly, hind limbs were dissected and homogenized in 0.05% SDS-polyacrylamide gel (Thermo Scientific) using an automated electrophoresis system (GE Healthcare, Hamilton, ON, Canada). The samples were suspended in 0.1 M phosphate buffer (pH 6.0) containing 0.05% each of protease inhibitors (Roche Diagnostics, Indianapolis, IN, USA) and 0.3 mM EDTA for 3 min. The supernatant was collected and the cells were analyzed using flow cytometry (Beckman Coulter). Five hundred thousand cells were analyzed/plate.

To confirm that MSCs remained in the bone marrow environment during the transplantation procedure, the cells were collected from the bone marrow and then serum-free for two months. MSCs were then treated for 1 month with dexamethasone (Sigma Aldrich, St. Louis, MO, USA) for 7 days to inhibit apoptosis. Media were collected and analyzed using FlowJo software (Tree Star Inc, Ashland, OR, USA).

To investigate the effect of the transplantation procedure on the cell division rate, the number of cells was determined by the cell density. MSCs were harvested from the hind limbs and transplanted into the marrow cavity of 8-week-old mice using a 2:1 ratio of MSCs/MSCs (Stratagene, La Jolla, CA, USA) for 8 months.

To evaluate the survival of transplanted MSCs, the cells were fixed in 4% paraformaldehyde in phosphate buffer saline (PBS) for 24 h and then stained with a fluorescent peroxidase-conjugated anti-rabbit antibody (Santa Cruz Biotechnology, Santa Cruz, CA, USA). At the conclusion of the 8-month study, MSCs were harvested for further analysis.

To monitor the long-term survival of MSCs *in vivo*, MSCs were harvested from human bone marrow (BM) and transplanted into 4-week-old mice for 8-month. MSCs were harvested for 7 days and then serum-free. Human bone marrow (BM) and marrow adipose tissue (BMAT) samples were obtained from the same donors (BM) and transplanted into 4-week-old mice for 8-month.

## references

- Sazo G, E R, Maenaka, Katsumi, Gu, Weiyong, et al. Fabrication of growth factor- and extracellular matrix-loaded, gelatin-based scaffolds and their biocompatibility with Schwann cells and dorsal root ganglia. *Biomaterials* 2013;p. 8529–8539.
- Singh, Pal S, Holdway, E J, Poss, D K. Regeneration of amputated zebrafish fin rays from de novo osteoblasts. *Developmental cell* 2012;p. 879–886.
- Singh, Pal S, Holdway, E J, Poss, D K. Regeneration of amputated zebrafish fin rays from de novo osteoblasts. *Developmental cell* 2012;p. 879–886.
- Cox, A J, Adow M, R A, Dinitz, E A, et al. A zebrafish SKIV2L2-enhancer trap line provides a useful tool for the study of peripheral sensory circuit development. *Gene expression patterns : GEP* 2012;p. 409–414.
- Lawrence, A P, Struhl, Gary, Casal, José. Planar cell polarity: one or two pathways? *Nature reviews Genetics* 2009;p. 555–563.
- Kallestad, M K, Mcloon, K L. Defining the Heterogeneity of Skeletal Muscle-Derived Side and Main Population Cells Isolated Immediately Ex Vivo. *Journal of cellular physiology* 2011;p. 676–684.
- Carkaci-Salli, N, Battula, S, Wang, X, et al. Gender specific regulation of tyrosine hydroxylase in Thy-1 knockout mice. *Journal of Neuroscience Research* 2013;p. 1583–1588.
- Cox, A J, Adow M, R A, Dinitz, E A, et al. A zebrafish SKIV2L2-enhancer trap line provides a useful tool for the study of peripheral sensory circuit development. *Gene expression patterns : GEP* 2012;p. 409–414.
- Geevarghese, Anita, Herman, M I. Pericyte-Endothelial Cross-Talk: Implications and Opportunities for Advanced Cellular Therapies. *Translational research : the journal of laboratory and clinical medicine* 2015;p. 296–306.
- Alcon, Andre, Bozkulak, Cagavi E, Qyang, Yibing. Regenerating functional heart tissue for myocardial repair. *Cellular and Molecular Life Sciences* 2012;p. 2635–2656.
- Leri, Annarosa, Kajstura, Jan, Anversa, Piero. Role of Cardiac Stem Cells in Cardiac Pathophysiology: A Paradigm Shift in Human Myocardial Biology. *Circulation Research* 2012;p. 941–961.
- Barrilleaux, Bonnie, Knoepfler, S P. Inducing iPSCs to Escape the Dish. *Cell stem cell* 2012;p. 103–111.
- Froehlich, Michael J, Seiliez, Iban, Gabillard, Charles J, et al. Preparation of Primary Myogenic Precursor Cell/Myoblast Cultures from Basal Vertebrate Lineages. *Journal of visualized experiments : JoVE* 2015;p. 323–325.
- Harkins, L A, Duri, Simon, Kloth, C L, et al. Chitosan–cellulose composite for wound dressing material. Part 2. Antimicrobial activity, blood absorption ability, and biocompatibility. *Journal of biomedical materials research Part B, Applied biomaterials* 2015;p. 1199–1206.
- Frakes, E A, Ferraiuolo, Laura, Phillips H, M A, et al. Microglia induce motor neuron death via the classical NF- $\kappa$ B pathway in amyotrophic lateral sclerosis. *Neuron* 2015;p. 1009–1023.
- Shao, Su J, Sierra, L O, Cohen, Richard, et al. Vascular Calcification and Aortic Fibrosis: A Bifunctional Role for Osteopontin In Diabetic Arteriosclerosis. *Arteriosclerosis, thrombosis, and vascular biology* 2012;p. 1821–1833.